

# Scattering phases in quantum dots: an analysis based on lattice models

A. Levy Yeyati<sup>1</sup> and M. Büttiker<sup>2</sup>

<sup>1</sup>Departamento de Física Teórica de la Materia Condensada CV, Universidad Autónoma de Madrid, E28049 Madrid, Spain

<sup>2</sup>Département de Physique Théorique, Université de Genève, CH-1211, Genève 4, Switzerland

## Abstract

The properties of scattering phases in quantum dots are analyzed with the help of lattice models. We first derive the expressions relating the different scattering phases and the dot Green functions. We analyze in detail the Friedel sum rule and discuss the deviation of the phase of the transmission amplitude from the Friedel phase at the zeroes of the transmission. The occurrence of such zeroes is related to the parity of the isolated dot levels. A statistical analysis of the isolated dot wave-functions reveals the absence of significant correlations in the parity for large disorder and the appearance, for weak disorder, of certain dot states which are strongly coupled to the leads. It is shown that large differences in the coupling to the leads give rise to an anomalous charging of the dot levels. A mechanism for the phase lapse observed experimentally based on this property is discussed and illustrated with model calculations.

## I. INTRODUCTION

Phase coherence is at the heart of most phenomena studied in mesoscopic physics. However, the behavior of the electronic wave-function phase *itself* in an actual quantum transport device had not been studied until recent years. In the case of quantum dots, investigations have been predominantly restricted to conductance measurements [1] which carry no information on the transmission phase. It was not until the experiments by Yacoby et al. [2] that the interest in phase behavior of quantum dots really started. In these experiments a quantum dot was embedded in one of the arms of an Aharonov-Bohm (AB) ring in an attempt to analyze the transmission phase evolution as a function of the dot gate voltage. Although these experiments were the first to demonstrate the presence of a coherent component in the current through a quantum dot in the Coulomb blockade regime, they failed to give the complete evolution of the phase. This limitation was explained [3] as a consequence of the phase locking (or phase rigidity) that occurs in a two terminal geometry. It was shown [3] that the AB effect in such geometry is characterized by a *parity*: as a function of the AB flux the conductance exhibits either a local maximum at zero flux (positive parity) or a local minimum (negative parity). Another intriguing feature of the experimental results was the

“parity conservation” over a large sequence of Coulomb blockade peaks, which reflected a similar evolution of the phase over each peak. The complete evolution of the phase could be obtained in a subsequent experiment by Schuster et al. [4] using a four terminal geometry. This experiment confirmed the expected evolution of the phase around the peaks and revealed that an abrupt jump of  $\pi$  occurs in the valleys between the peaks.

Since 1995 several theoretical efforts have been devoted to explain these observations [3,5–8,10,9,11–17]: Ref. [3] proposed a screening effect, Ref. [5] alluded to dot degeneracies, Refs. [6,9,11] associated the observed effect to an asymmetric deformation of the dot which leads to repeated charging of the same dot level and Ref. [16] pointed out some special properties of the dot states in a semi-chaotic situation (this mechanism will be further analyzed in the present work). In spite of all these efforts there is still the feeling that a more fundamental explanation is lacking. Each one of the proposed mechanisms can be criticized as relying on some particular assumptions. Only the approximate sum rule proposed recently in Ref. [17] is supposed to be valid in a generic (chaotic) situation. However, there is still no experimental evidence of the near resonance phase-lapse predicted by this mechanism.

On the other hand, the phase problem affects our knowledge on generic properties of scattering phases. One fundamental relation, invoked in Ref. [3] in connection to this problem, is the Friedel sum rule which relates the phase of the eigenvalues of the scattering matrix to the charge accumulated in the dot region. Being related to the dot charge, the Friedel phase is a continuous function of the system parameters and cannot exhibit an abrupt behavior like the one found in the experiments by Schuster et al. [4]. However, as pointed out recently by Lee [18] and Taniguchi and one of the authors [19] the phase of the transmission amplitude can depart from the Friedel phase and exhibit a non-analytic behavior at the points where the modulus of the transmission vanishes. It is thus interesting to study the general conditions for the occurrence of zeroes in the transmission through a quantum dot.

The aim of this paper is to investigate the behavior of the different scattering phases in quantum dots with the help of lattice models. These type of models allow to describe a dot of arbitrary shape and to study the influence of disorder [20]. We shall first derive the expressions for the different scattering phases in terms of Green functions. These expressions allow to relate the occurrence of zeroes in the transmission with the parity of the isolated dot wave-functions. We also study the statistical properties of the dot wave-functions in a disordered quantum dot, showing explicitly the absence of significant correlations in the chaotic case. On the other hand, as suggested in Ref. [16], for weak disorder one can identify certain dot levels which are much more strongly coupled to the leads than average. We shall show that in this situation the dot levels are populated in an anomalous way as a function of gate voltage. We shall finally discuss the possible role of this type of correlation effects in the phase problem.

The outline of the paper will be the following: In section II we introduce a generic lattice model for a Quantum Dot coupled to single-moded leads. In section III we derive the expressions for the different scattering phases in terms of Green functions. We discuss in particular the Friedel sum rule and the relation of the Friedel phase to the phase of the transmission amplitude. In section IV we study the conditions for the occurrence of zeroes in the transmission and show that they are independent of the strength of the coupling to the leads. The statistical properties of the isolated dot wave-functions are analyzed in section V. Finally, in section VI we discuss the role of electron correlation effects. We end the paper

with some conclusions and final remarks.

## II. GENERIC LATTICE MODEL

As a model for a two dimensional quantum dot we consider a collection of  $N$  sites on a square lattice (see Fig. 1). This model can represent a dot of arbitrary shape. The electrons in the dot are described by a tight-binding Hamiltonian with site energies  $\epsilon_i$  and a constant hopping element  $t$  coupling nearest-neighbors only. ( $t$  will be taken as the unit of energy). The site energies are allowed to vary following an imposed electrostatic confining potential and/or randomly in order to study the influence of disorder.

On the other hand, electron-electron interactions can be included within the constant charging energy model by adding a term  $V_{coul} = E_C(N_{dot} - CV_g/e)^2$ , where  $N_{dot}$  is the mean number of electrons in the dot, to the one-electron Hamiltonian. Its effect will be discussed in section VI.

We shall consider that the dot is coupled to electron reservoirs by two one-dimensional leads as depicted in Fig. 1. We may assume that the coupling to the left and right leads is restricted to two sites labeled by 1 and  $N$  respectively. The first site on each lead are connected to these two sites on the dot by hopping elements  $t_L$  and  $t_R$  respectively. As will be discussed later, this situation can be easily generalized to the case where the first sites on the leads are connected to several sites on the dot (this multiple connection is illustrated in Fig. 1 by the dashed lines).

## III. SCATTERING PHASES AND GREEN FUNCTIONS

The electronic properties of lattice models are conveniently given in terms of Green functions. We need to introduce the retarded and advanced Green operators given by

$$\hat{G}^{r,a}(\omega) = [\omega - \hat{H}_{dot} - \hat{\Sigma}^{r,a}(\omega)]^{-1}, \quad (1)$$

where  $\hat{H}_{dot}$  is the one-electron part of the isolated dot Hamiltonian and  $\hat{\Sigma}^{r,a}$  is the (retarded, advanced) self-energy operator describing the coupling of the dot to the leads. In a Fermi-liquid like description, the self-energy should also contain terms accounting for electron-electron interactions [21]. We shall postpone its discussion to section VI and concentrate on the one-electron properties of the quantum dot until then. When the coupling to the leads is localized at sites 1 and  $N$  we have

$$\Sigma_{l,m}^{r,a}(\omega) = \delta_{l,j_\alpha} \delta_{m,j_\alpha} t_\alpha^2 g_\alpha^{r,a}(\omega), \quad (2)$$

where  $\alpha = L, R$ ,  $j_L = 1$ ,  $j_R = N$  and  $g_\alpha^{r,a}$  are the local Green functions at the semi-infinite one-dimensional leads.

In terms of the Green operator one can express the dot total density of states  $\rho(\omega)$  as

$$\rho(\omega) = \frac{1}{2\pi i} \text{Tr} [\hat{G}^a(\omega) - \hat{G}^r(\omega)] = \frac{1}{\pi} \text{Im} \text{ Tr} [\hat{G}^a(\omega)]. \quad (3)$$

We shall now discuss the connection of this quantity to the scattering matrix  $\hat{S}(\omega)$ , defined in terms of Green functions by means of the generalized Fisher-Lee relations [22]

$$S_{\alpha,\beta}(\omega) = \delta_{\alpha,\beta} - 2i\sqrt{\Gamma_\alpha\Gamma_\beta}G_{j_\alpha,j_\beta}^r(\omega), \quad (4)$$

where we have introduced the tunneling rates  $\Gamma_\alpha = t_\alpha^2 \text{Im}g_\alpha^a$ . The unitarity of  $\hat{S}$  can be readily shown (see appendix A). We start by defining the quantity  $\theta_F$  as

$$\theta_F(\omega) = \text{ImLnDet} [\omega - \hat{H}_{dot} - \hat{\Sigma}^a(\omega)]. \quad (5)$$

The derivative with respect to the energy of  $\theta_F$  is then given by

$$\frac{\partial\theta_F}{\partial\omega} = \text{ImTr} \left[ \hat{G}^a \left( 1 - \frac{\partial\hat{\Sigma}^a}{\partial\omega} \right) \right]. \quad (6)$$

Thus, in the case when the energy dependence of the self-energy can be neglected one obtains the identity

$$\frac{\partial\theta_F}{\partial\omega} = \pi\rho(\omega). \quad (7)$$

This case corresponds to a particular type of leads, having a large density of states, which can screen any deviation from charge neutrality induced by the presence of the dot. This type of leads can be called “non-polarizable leads”.

On the other hand, it can be show (see appendix B) that  $\theta_F$  can be expressed in terms of the scattering matrix  $\hat{S}$  as

$$\theta_F(\omega) = \frac{1}{2i} \text{lnDet} [\hat{S}(\omega)] \quad (8)$$

and thus one obtains a relation between the dot total density of states and the derivative of the scattering matrix with respect to the energy

$$\rho(\omega) = \frac{1}{2\pi i} \frac{\partial}{\partial\omega} \text{lnDet} [\hat{S}(\omega)]. \quad (9)$$

Then, by integrating this expression up to the Fermi energy, we obtain the generalized Friedel sum rule

$$N_{dot} = \frac{1}{\pi} \theta_F(E_F). \quad (10)$$

We see that  $\theta_F$  is an important scattering phase. As it is related to the dot charge it should be a continuous function of the energy. It has also a simple relation to the eigenvalues of the scattering matrix. Due to the unitarity of  $\hat{S}$  its eigenvalues are of the form  $e^{2i\xi_{1,2}}$  and thus  $\theta_F = \xi_1 + \xi_2$ .

It should be emphasized that relation (10) holds only for the case of non-polarizable leads. For a more general case one should include also the charge induced on the leads in the Friedel sum rule. The deviation between the dot total density of states and the derivative of the Friedel phase with respect to energy has also been pointed out by Gasparian et al.

[23] who analized the connection between densities of states and the scattering matrix for continuous models. In particular Eq. (14) in [23] can be written as

$$\frac{\partial \theta_F}{\partial \omega} = \pi \rho(\omega) - \text{Im} \left( \frac{s_{L,L} + s_{R,R}}{4\omega} \right) \quad (11)$$

which coincides with our Eq. (6) provided that we make the approximation

$$\frac{\partial \hat{\Sigma}}{\partial \omega} \approx \frac{i \text{Im} \hat{\Sigma}}{2\omega}. \quad (12)$$

Another scattering phase which is relevant for the interference phenomena observed in the experiments is the phase of the transmission amplitude  $\theta_t = \arg S_{LR}$ . In some particular cases (for instance in a one-dimensional problem)  $\theta_F$  and  $\theta_t$  coincide. However, as noticed recently by some authors [18,19], they are in general different. While  $\theta_F$  is a continuous function,  $\theta_t$  may not be defined at certain energies where the transmission vanishes. In order to be more precise, one can parametrize a general scattering matrix as

$$\hat{S} = \begin{pmatrix} ie^{i(\theta+\varphi_1)} \sin \phi & e^{i(\theta+\varphi_2)} \cos \phi \\ e^{i(\theta-\varphi_2)} \cos \phi & ie^{i(\theta-\varphi_1)} \sin \phi \end{pmatrix}. \quad (13)$$

with real phases  $\theta$ ,  $\varphi_1$ ,  $\varphi_2$  and  $\phi$ . It is then easy to show that  $\theta_F = \theta + \pi/2$ . On the other hand, when time reversal symmetry holds one has  $S_{LR} = S_{RL}$  and thus  $\varphi_2 = 0$ , in which case the argument of the transmission amplitude is related to  $\theta_F$  by

$$\theta_t = \theta_F + \pi \Theta(\cos \phi) - \frac{\pi}{2}, \quad (14)$$

where  $\Theta(x)$  is the step function. Therefore,  $\theta_t$  exhibits jumps of  $\pi$  each time  $\cos \phi$  changes sign, i.e. at the points where there is a zero of the transmission. At these points the phase of the transmission amplitude deviates from the Friedel phase. Notice that the abrupt jump of  $\pi$  of the phase of the AB oscillations between consecutive resonances is a central feature of the experimental results of Schuster et al. [4]. We thus conclude that the study of the occurrence of zeroes of the transmission is essential to understand the experimentally observed behavior.

#### IV. CONDITIONS FOR ZEROES OF THE TRANSMISSION

Within lattice models one can establish precise conditions for the occurrence of zeroes in the transmission amplitude through the dot. According to the Fisher-Lee relations the condition for having a zero in  $S_{LR}$  at energy  $E_0$  is that  $G_{1N}^r(E_0) = 0$ . This is gives

$$G_{1N}^r(E_0) = \frac{C_{1N}(E_0 - \hat{H}_{dot} - \hat{\Sigma}^r(E_0))}{\text{Det}(E_0 - \hat{H}_{dot} - \hat{\Sigma}^r(E_0))} = 0, \quad (15)$$

where  $C_{ij}(\hat{A})$  denotes the cofactor of the element  $i, j$  in the matrix  $\hat{A}$ . It is easy to see that the polynomial in the numerator is real and does not depend on the self-energy coupling of the dot to the leads at sites 1 and  $N$ . This is a direct consequence of having the coupling

to the leads localized at these sites. We can thus reduce the condition for the zeroes, Eq. (15), to the simpler expression

$$C_{1N} (E_0 - \hat{H}_{dot}) = 0. \quad (16)$$

Eq. (16) clearly shows that the zeroes of the transmission are characteristic of the isolated dot structure and do not depend on the strength of the coupling to the leads. This is illustrated in Fig. 2 where the transmission for a 5x5 sites dot is shown for varying values of  $\Gamma$  within an energy range having a zero. One can observe that while the shape of the transmission varies substantially, the position of the zero is not affected.

This property allows one to relate the zeroes of the transmission to the wavefunctions of the isolated dot. In the weak coupling limit one can approximate  $G_{1N}$  as

$$G_{1N}^a \approx \sum_n \frac{\psi_1^n \psi_N^n}{\omega - \lambda_n - i\Gamma_L(\psi_1^n)^2 - i\Gamma_R(\psi_N^n)^2}, \quad (17)$$

where  $\lambda_n$  and  $\psi_j^n$  denote the eigenvalues and the amplitudes of the corresponding wavefunction for the isolated dot. The condition to have a zero between two consecutive eigenvalues  $\lambda_n, \lambda_{n+1}$  is then simply given by  $\psi_1^n \psi_N^n \psi_1^{n+1} \psi_N^{n+1} > 0$ .

We can now identify the sign of  $\psi_1^n \psi_N^n$  as the *parity* of the corresponding dot wavefunction. By this reasoning we conclude that there should be a zero of the transmission in between dot states with the same parity *regardless of the strength of the coupling to the leads*.

In real systems inelastic scattering would prevent the occurrence of exact zeroes in the transmission. This situation can be described within our model by additional leads coupled to the dot as voltage probes [24]. This effect is discussed in the next subsection.

### A simple example

A simple example which already exhibits a zero in the transmission amplitude is the case of a four sites sites dot, i.e.  $N = 4$ . In this model sites 1 and 4 are the ones coupled to the leads. Sites 2 and 3 are coupled to sites 1 and 4 by hopping elements  $t$  and we take the site energies on 1 and 4 as  $\epsilon_1 = \epsilon_4 = 0$ . The transmission amplitude for such model is given by

$$S_{LR} = -2i\sqrt{\Gamma_L \Gamma_R} \frac{2t^2(\omega - \bar{\epsilon})}{(\omega + i\Gamma_L)(\omega + i\Gamma_R)(\omega - \epsilon_2)(\omega - \epsilon_3) - 4t^2(\omega - \bar{\epsilon})(\omega + i\bar{\Gamma})}, \quad (18)$$

where  $\bar{\epsilon} = (\epsilon_2 + \epsilon_3)/2$  and  $\bar{\Gamma} = (\Gamma_L + \Gamma_R)/2$ .

For weak coupling and  $|\epsilon_2 - \epsilon_3| \gg t$  the transmission has two well resolved resonances at  $\omega \simeq \epsilon_{2,3}$ . The modulus and the phase of  $S_{LR}$  are shown in Fig. 3. As can be observed the phase of the transmission exhibits a similar evolution around each resonance. At the point  $\omega = \bar{\epsilon}$  there is a zero of the transmission and its phase exhibits an abrupt jump of  $\pi$ . From Eq. 18 it is clear that the zero is not dependent on the strength of the coupling to the leads.

Inelastic scattering can be simulated by additional voltage probes coupled to sites 2 and 3. Let us denote by  $\Gamma_{inel}$  the coupling to the additional leads. It is easy to see that the zero of the transmission now moves away from the real energy axis to  $\bar{\epsilon} + i\Gamma_{inel}$ . The jump in the phase of the transmission becomes smaller than  $\pi$  and it is no longer abrupt but has a finite width given by  $\Gamma_{inel}$ . The width of the phase jump can thus be taken as a measure of broadening of the dot levels due to inelastic scattering.

## V. STATISTICAL ANALYSIS OF THE TRANSMISSION PHASE

According to the discussion of the previous section, the occurrence of zeroes in the transmission (and the associated jump in the transmission phase) is related to the parity of the isolated dot wavefunctions on consecutive levels. In a similar way as done by many authors for analyzing the mesoscopic conductance fluctuations of quantum dots in the Coulomb blockade regime [25], the parity should be studied statistically over many realizations of the dot potential.

In order to search for correlations of the parity of the dot wavefunctions we have numerically diagonalized dot lattice models up to  $30 \times 30$  sites. The confining potential is assumed to have the form of an isotropic parabola with curvature  $\alpha$ . We have investigated the influence of disorder and also the influence of different models for coupling the dot to the leads.

Figure 4a shows the spacing distribution between consecutive levels for various values of the disorder strength  $W$  and  $\alpha = 0.01$  (in units of  $t/a^2$ , where  $a$  is the lattice spacing). One can notice that the distribution approaches the the Wigner distribution [26]

$$p(s) = \frac{\pi}{2} s \exp\left[-\frac{\pi}{4}s^2\right]$$

(plotted as a full line in Fig. 4a) as the disorder strength increases. This agreement suggests that our results for  $W > 1$  should be well described by random matrix theory.

For analyzing correlations in the parity of the wavefunctions we plot in Fig. 4b the probability to find consecutive levels with the same parity as a function of level spacing. As can be observed, this probability is almost constant as a function of level spacing. Although the probability is slightly larger than 0.5 for weak disorder ( $W = 0.5$ ) it approaches 0.5 as the disorder increases. This behavior indicates that correlations in the parity are negligible within this model.

The previous results correspond to the case where the dot is coupled to the leads at sites 1 and  $N$ , and thus the parity of the wavefunctions is given by  $\arg(\psi_1^n \psi_N^n)$ . This situation can be generalized to the case where many dot sites are coupled to each lead as indicated by the dotted lines in Fig. 1. We shall assume that both leads are coupled to the same number  $N_{leads}$  of neighboring sites on each side of the dot. In this case the parity will be given by  $\arg(\sum_{j_L, j_R} \psi_{j_L}^n \psi_{j_R}^n)$ , where  $j_{L,R}$  denote the sites coupled to the left and right lead respectively. It should be emphasized that the conditions for the occurrence of zeroes discussed in section IV remains valid in this case, the first sites on the leads  $L$  and  $R$  playing the role of sites 1 and  $N$ .

In Fig. 5 we show the total probability to find consecutive levels with the same parity as a function of  $N_{leads}$  and different values of the disorder strength  $W$ . For  $W = 0.5$  one can notice a slight decrease of the probability for increasing  $N_{leads}$ . The probability nevertheless remains always close to 0.5 indicating the absence of significant parity correlations even when changing the model for coupling the dot to the leads.

These results demonstrate that it is very unlikely to find a large sequence of dot levels with the same parity and consequently the difficulty to account for the experimental results of Ref. [4] within a one-electron model. There are, however, some peculiarities of the dot states in the limit of weak disorder which can give rise to correlation effects as discussed in

the next section. These correlation effects are associated with certain dot states which are strongly coupled to the leads as discussed below.

The coupling strength  $\alpha_n = |\sum_{j_L, j_R} \psi_{j_L}^n \psi_{j_R}^n|$  is shown in figure 6 as a function of the level number for the case  $N_{leads} = 5$  and different values of  $W$ . In the case of extended contacts to the leads and weak disorder one can clearly distinguish states which are more strongly coupled to the leads than the average. For the case  $W = 0.5$ , this states are indicated by arrows in Fig. 6. One can notice by their level number (67,79,92,106,..) that they appear in a well defined sequence, corresponding to the shell structure of states in the isotropic 2D harmonic oscillator. Contour plots of the wavefunctions with level number 67 and the next three levels are shown in Fig. 7. Although they correspond to nearly degenerate levels only the first one is strongly coupled to the leads.

## VI. EFFECTS DUE TO COULOMB INTERACTIONS

Up to now we have neglected interactions and concentrated on the one-electron properties of the dot. As commented in section II, electron-electron interactions can be included by means of the constant charging energy model. Within the traditional description of Coulomb blockade in quantum dots based on simple master equations [27] the main role of the charging energy is to open a gap between consecutive dot levels, dot states being populated according to the isolated dot ground state for each number of electrons. Within this picture, the evolution of the phase over a sequence of dot resonances will be fixed by the parity of the corresponding one-electron dot states. As discussed in the previous section, the parity of one-electron dot states does not exhibit significant correlations and therefore this picture is unable to account for the experimental results of Ref. [4].

The situation may change drastically when taking into account the finite coupling to the leads beyond lowest order perturbation theory. In this case correlation effects may lead to a population of the dot levels different to the one predicted by simple master equations. This possibility was recently pointed out by Silverstrov and Imry [16] and advanced as an explanation of the experimental results on the phase of the transmission through a quantum dot. The mechanism proposed by these authors would take place when there is a strongly coupled dot level followed by nearly degenerate weakly coupled levels. This situation is characteristic for the case of weak disorder discussed in the previous section.

The basic mechanism proposed by Silverstrov and Imry can be understood by considering a simple four sites problem with two (spinless) electrons. We shall assume that two of the sites correspond to the dot levels and the other two represent the left and right leads. Let us call  $\epsilon_1$  and  $\epsilon_2$  the one-electron energies of the isolated dot levels and  $\Delta = \epsilon_2 - \epsilon_1 > 0$  the spacing between them. The lower level is symmetrically coupled to the leads by effective hopping elements  $t_{1L} = t_{1R} = T$  which are much larger than the ones corresponding to the upper level  $t_{2L} = t_{2R} = t$ . The energy levels on the leads sites are taken as zero. Let us analyze how the dot levels are populated as the gate voltage shift down the energy levels from  $\epsilon_1, \epsilon_2 \gg 0$  to  $\epsilon_1, \epsilon_2 \ll 0$ .

Finding the ground state of this problem requires in principle to diagonalize the  $6 \times 6$  matrix corresponding to the system Hamiltonian in the basis  $|n_1 n_2 n_L n_R\rangle$  where  $(n_1, n_2)$  are the occupation numbers for the dot levels and  $(n_L, n_R)$  correspond to the leads. The problem can, however, be reduced by a basis change in which we replace the states with one

electron in the leads by its symmetric and anti-symmetric combination, i.e  $|1010\rangle$ ,  $|1001\rangle$ ,  $|0110\rangle$  and  $|0101\rangle$  are replaced by  $(|1010\rangle \pm |1001\rangle)/\sqrt{2}$  and  $(|0110\rangle \pm |0101\rangle)/\sqrt{2}$ . In this way, the initial  $6 \times 6$  matrix is reduced into two  $3 \times 3$  blocks: one block corresponds to the empty dot states which couples to the anti-symmetric combinations and the other to the doubly occupied dot state coupled to the symmetric combinations, having the form

$$H^s = \begin{pmatrix} \epsilon_1 + \epsilon_2 + E_c & \sqrt{2}T & \sqrt{2}t \\ \sqrt{2}t & \epsilon_2 & 0 \\ \sqrt{2}t & 0 & \epsilon_1 \end{pmatrix} \quad H^a = \begin{pmatrix} \epsilon_1 & 0 & \sqrt{2}T \\ 0 & \epsilon_2 & \sqrt{2}t \\ \sqrt{2}T & \sqrt{2}t & 0 \end{pmatrix}$$

In the limit  $\Delta \rightarrow 0$ , i.e.  $\epsilon_2 \rightarrow \epsilon_1 = -V_g$  the ground state for each symmetry is given by

$$\lambda^s = \frac{-3V_g + E_c}{2} - \sqrt{\left(\frac{-V_g + E_c}{2}\right)^2 + 2(T^2 + t^2)}$$

$$\lambda^a = \frac{V_g}{2} - \sqrt{\left(\frac{V_g}{2}\right)^2 + 2(T^2 + t^2)}$$

When  $V_g \ll 0$  the system starts in the anstisymmetric ground state and the charge of the dot levels evolve with  $V_g$  according to

$$\langle n_1 \rangle = \frac{2T^2}{(V_g + \lambda^a)^2 + 2(T^2 + t^2)} \quad \langle n_2 \rangle = \frac{2t^2}{(V_g + \lambda^a)^2 + 2(T^2 + t^2)}$$

which shows that the dot levels start populating when  $-V_g \sim T$ . However, as  $t \ll T$ , the charge in the weakly coupled level will be negligible as compared to the strongly coupled one.

At  $V_g = E_c/2$  there is a crossing between  $\lambda^a$  and  $\lambda^s$ . As a result the symmetric ground state becomes more stable and the charge on each dot level is now given by

$$\langle n_1 \rangle = \frac{2t^2 + (V_g + \lambda^s)^2}{(V_g + \lambda^s)^2 + 2(T^2 + t^2)}, \quad \langle n_2 \rangle = \frac{2T^2 + (V_g + \lambda^s)^2}{(V_g + \lambda^s)^2 + 2(T^2 + t^2)}$$

Thus, when crossing  $V_g = E_c/2$  the charge on the strongly coupled state goes from  $\sim T^2/(T^2 + t^2)$  to  $\sim t^2/(T^2 + t^2)$  while the charge on the weakly coupled level does the opposite evolution (we neglect small corrections of order  $(T/E_c)^2$ ). We see that nearly one electron is transferred from the strongly coupled level to the weakly coupled one in the middle of the charging curve, the total charge in the dot remaining constant (up to order  $(T/E_c)^2$ ). The strongly coupled level is again filled when  $V_g$  is close to  $E_c$ . The situation is similar for finite  $\Delta \ll T$ , the abrupt jump is also present but shifted to  $V_g \sim E_c/2 + \Delta$ .

A more realistic description of the actual situation requires the inclusion of many sites to represent both the leads and the dot levels. One would need a large number of sites in order to simulate a continuous density of states on the leads. Using Lanczos method we are able to numerically diagonalize interacting systems with up to 16 sites and 8 electrons. The dot levels charge as a function of gate voltage for a systems with 6 sites on a line for representing each lead and 4 sites for representing the dot levels, is shown in Fig. 8. The dot levels are coupled symmetrically to the leads by hopping parameters  $t_1 = 0.1$  and  $t_2 = t_3 = t_4 = 0.02$

(all energies in units of the charging energy  $E_c$ ) while the hopping parameter within the leads is taken as 0.1. The weakly coupled levels lie at 0.025, 0.030, and 0.035 respectively above the strongly coupled level. As can be observed, the strongly coupled level is repeatedly charged and discharged in a similar way as for the simple four sites model. One can notice, however, that the jumps in the charge of the strongly coupled level are not so much abrupt and become progressively less pronounced.

The next question is how this particular charging of the dot levels affects the transmission amplitude and its phase. In order to obtain the transmission through the interacting dot we map this finite size cluster into an effective non-interacting system with the same charge on each dot level for each value of the gate voltage. In this effective system we use the same hopping parameters as in the cluster calculation but replace the leads by infinite one-dimensional chains. The effective dot levels are determined self-consistently to get the correct level charges. The phase of the transmission amplitude and the transmission probability thus obtained are shown in Fig. 9. As expected, the phase follows closely the charge of the strongly coupled level. It should be remarked that this behavior is not dependent on the parity of the weakly coupled levels. On the other hand, the transmission probability exhibits broad peaks that can be associated with the repeated charging of the strongly coupled level together with narrow satellite peaks corresponding to the charging of the weakly coupled levels. These narrow peaks lie closer to the broader peaks as the cycle number increases. In the fourth cycle the narrow peak can hardly be resolved.

## VII. CONCLUSIONS AND FINAL REMARKS

To summarize, we have analyzed the behavior of scattering phases in quantum dots using lattice models. We have first studied the definition of the different scattering phases in terms of Green functions. We have shown that abrupt jumps of  $\pi$  in the phase of the transmission amplitude are associated with the occurrence of transmission zeroes. Then, we have shown that within lattice models and assuming single mode leads the zeroes are independent of the strength of the coupling to the leads [28]. This property allows us to relate the occurrence of a zero with the parity of consecutive dot states in the isolated dot.

We have studied the statistical properties of the isolated dot states as a function of the disorder strength. This analysis reveals that there are no significant parity correlations between consecutive dot levels. For moderate disorder there appear states which are much more strongly coupled to the leads than the average. We have studied charging effects in this situation using exact diagonalization of small clusters. We have shown that the dot resonances as a function of gate voltage may correspond to the strongly coupled level through several cycles.

The viability of this mechanism as a possible explanation of the “phase problem” deserves further discussion. The presence of strongly coupled levels followed by many weakly coupled levels is a reminiscent of the integrable case which gradually disappears for increasing disorder (see Fig. 6). In this sense, the mechanism is not universal as it would not hold for a fully chaotic quantum dot. Thus, this mechanism could be tested experimentally by leading the dot into a fully chaotic situation (using, for instance additional gates to distort the dot shape, as in Ref. [29]). On the other hand, the transmission as a function of gate voltage exhibits narrow satellite peaks close to the broader Coulomb blockade peaks (see

Fig. 9) which are not observed experimentally. Being so narrow these peaks could be easily washed out by thermal broadening or due to the finite bias voltage used in the measurements. Of course if certain narrow peaks are not resolved in the experiment, a number of additional scenarios might account for parity conservation, even within a non-interacting picture. Differing parity conserving scenarios can then still be distinguished according to their phase evolution pattern. It is very unlikely that a non-interacting theory can generate a phase evolution like that of Fig. 9 which resembles closely that seen in the experiments.

One should also comment about the role of spin, not included in the present analysis. At very low temperatures spin degeneracy would lead to a Kondo effect. This effect has been recently observed experimentally [30] but in somewhat smaller quantum dots and would be reflected in the phase behavior as a plateau at  $\sim \pi/2$  in between a pair of resonances corresponding to the same dot level [15,31]. At temperatures larger than the Kondo temperature spin degeneracy could at most account for the similar phase behavior over two consecutive dot resonances. Other spin effects, like Hund's rule require almost perfect symmetry leading to orbital degeneracy and so far have been observed only in ultrasmall quantum dots [32].

To conclude, we point out that our analysis has been restricted to the case of single-moded leads. This is an assumption which has been implicitly been used in all the theoretical models of the problem following the characterization of the experimental set up given in Ref. [4]. Nevertheless, the analysis of what would be measured in a multichannel situation is of interest and deserves further theoretical investigation.

## ACKNOWLEDGMENTS

The authors would like to thank T. Taniguchi for fruitful discussions. One of us (ALY) also thanks discussions with F. Flores and J.A. Vergés. This work has been partially supported by the Spanish CICYT under contract PB97-0044 and the Swiss National Science Foundation.

## Appendix A

We show in this appendix the unitarity of the scattering matrix defined from the Fisher-Lee relations. One has

$$\begin{aligned} (\hat{S}^\dagger \hat{S})_{11} &= |1 - 2i\Gamma_L G_{11}^r|^2 + 4\Gamma_L \Gamma_R |G_{1N}^r|^2 \\ (\hat{S}^\dagger \hat{S})_{12} &= -2i\sqrt{\Gamma_L \Gamma_R} [(1 + 2i\Gamma_L G_{11}^a) G_{1N}^r - G_{1N}^a (1 - 2i\Gamma_R G_{NN}^r)], \end{aligned} \quad (19)$$

and similar expressions for  $(\hat{S}^\dagger \hat{S})_{21}$  and  $(\hat{S}^\dagger \hat{S})_{22}$ . These elements can be rewritten as

$$\begin{aligned} (\hat{S}^\dagger \hat{S})_{11} &= 2i\Gamma_L [G_{11}^a - G_{11}^r - 2i\Gamma_L |G_{11}^a|^2 - 2i\Gamma_R |G_{1N}^a|^2] + 1 \\ (\hat{S}^\dagger \hat{S})_{12} &= -2i\sqrt{\Gamma_L \Gamma_R} [G_{1N}^r - G_{1N}^a + 2i\Gamma_L G_{11}^a G_{1N}^r + 2i\Gamma_R G_{1N}^a G_{NN}^r]. \end{aligned} \quad (20)$$

It is now easy to show that the expressions between brackets vanish identically. This fact is a consequence of the identity

$$\hat{G}^a - \hat{G}^r = \hat{G}^a [\hat{\Sigma}^a - \hat{\Sigma}^r] \hat{G}^r \quad (21)$$

which follows from the definition of the Green operator. Taking the matrix elements (1,1) and (1,N) one finds

$$\begin{aligned} G_{11}^a - G_{11}^r &= 2i\Gamma_L|G_{11}^a|^2 + 2i\Gamma_R|G_{1N}^a|^2 \\ G_{1N}^a - G_{1N}^r &= 2i\Gamma_L G_{11}^a G_{1N}^r + 2i\Gamma_R G_{1N}^a G_{NN}^r \end{aligned} \quad (22)$$

## Appendix B

We show in this appendix that  $2i\theta_F = \text{lnDet}[S]$ . First notice that

$$\theta_F = \text{ImlnDet} [\omega - \hat{H}_{dot} - \Sigma^a] = \frac{1}{2i} \text{lnDet} [(\omega - \hat{H}_{dot} - \Sigma^a) \hat{G}^r]. \quad (23)$$

From the definition of the Green operator one can rewrite this expression as

$$\theta_F = \frac{1}{2i} \text{lnDet} [1 + (\Sigma^r - \Sigma^a) G^r]. \quad (24)$$

Finally, using that  $(\Sigma^r - \Sigma^a)_{i,j} = -2i\Gamma_L\delta_{i,1}\delta_{j,1} - 2i\Gamma_R\delta_{i,N}\delta_{j,N}$ , one can easily check that

$$\theta_F = \frac{1}{2i} \text{lnDet} [S]. \quad (25)$$

## REFERENCES

- [1] For a review see L.P. Kouwenhoven, C.M. Marcus, P.L. McEuen, S. Tarucha, R.M. Westervelt and N.S. Wingreen, Proceedings of a NATO ASI on Mesoscopic Electron Transport, edited by L. Sohn, L.P. Kouwenhoven and G. Schön (Kluwer, 1997).
- [2] A. Yacoby, M. Heiblum, D. Mahalu, V. Umansky and H. Shtrikman, Phys. Rev. Lett. **74**, 4047 (1995).
- [3] A. Levy Yeyati and M. Büttiker, Phys. Rev. B **52**, R14360 (1995).
- [4] R. Schuster, E. Buks, M. Heiblum, D. Mahalu, V. Umansky and H. Shtrikman, Nature **385**, 417 (1997).
- [5] C. Bruder, R. Fazio and H. Schoeller, Phys. Rev. Lett. **76**, 114 (1996).
- [6] G. Hackenbroich and H. A. Weidenmüller, Phys. Rev. Lett. **76**, 110 (1996).
- [7] A. Yacoby, R. Schuster and M. Heiblum, Phys. Rev. B **53**, 9583 (1996).
- [8] P. S. Deo and A. M. Jayannavar, Mod. Phys. Lett. B **10**, 787 (1996).
- [9] G. Hackenbroich and H. A. Weidenmüller, Phys. Rev. B **53**, 16379 (1996).
- [10] Y. Oreg and Y. Gefen, Phys. Rev. B **55**, 13726 (1997).
- [11] G. Hackenbroich and H. A. Weidenmüller, Europhys. Lett, **38** (2), 129 (1997).
- [12] H. Xu and W. Sheng, Phys. Rev. B **57**, 11903 (1998).
- [13] C. -Mo Ryu and S. Y. Cho, Phys. Rev. B **58**, 3572 (1998).
- [14] R. Baltin, Y. Gefen, G. Hackenbroich and H. A. Weidenmüller, cond-mat/9807286.
- [15] K. Kang, cond-mat/9811354.
- [16] P. G. Silvestrov and Y. Imry, cond-mat/9903299.
- [17] R. Baltin and Y. Gefen, Phys. Rev. Lett. **83**, 5094 (1999).
- [18] H.-W. Lee, Phys. Rev. Lett. **82**, 2223 (1999).
- [19] T. Taniguchi and M. Büttiker, Phys. Rev. B **60**, 13814 (1999).
- [20] J.A. Vergés, E. Cuevas, M. Ortúñoz and E. Louis, Phys. Rev. B **58**, R10143 (1998).
- [21] A Fermi-liquid like description of quantum dots valid from the Kondo to the Coulomb blockade regimes has been presented in A. Levy Yeyati, F. Flores and A. Martín-Rodero, Phys. Rev. Lett. **83**, 600 (1999).
- [22] D.S. Fisher and P.A. Lee, Phys. Rev. B **23**, 6851 (1981).
- [23] V. Gasparian, T. Christen and M. Büttiker, Phys. Rev. A **54**, 4022 (1996).
- [24] M. Büttiker, IBM J. Res. Develop. **32**, 317 (1988).
- [25] R. Jalabert, A.D. Stone and Y. Alhassid, Phys. Rev. Lett. **68**, 3468 (1992).
- [26] M.L. Metha *Random Matrices* (Academic Press, San Diego 1991).
- [27] C.W.J. Beenakker, Phys. Rev. B **44**, 1644 (1991).
- [28] These results are not dependent on any particular assumption about the lattice model like band filling, lattice size, etc. We thus expect that they remain valid also for a continuous model.
- [29] J.A. Folk, S.R. Patel, S.F. Godijn, A.G. Huibers, S.M. Cronenwett, C.M. Marcus, K. Campman and A.C. Gossard, Phys. Rev. Lett. **76**, 1699 (1996).
- [30] D. Goldhaber-Gordon, H. Shtrikman, D. Mahalu, D. Abusch-Maggder, U. Meirav and M.A. Kastner, Nature **391**, 156; (1998); S.M. Cronenwett, T.H. Oosterkamp and L.P. Kouwenhoven, Science **281**, 540 (1998).
- [31] J. von Delft, U. Gerland, T. Costi and Y. Oreg, cond-mat 9909401.
- [32] S. Tarucha, D.G. Austing, T. Honda, R.J. van der Hage and L.P. Kouwenhoven, Phys. Rev. Lett. **77**, 3613 (1996).

## FIGURES

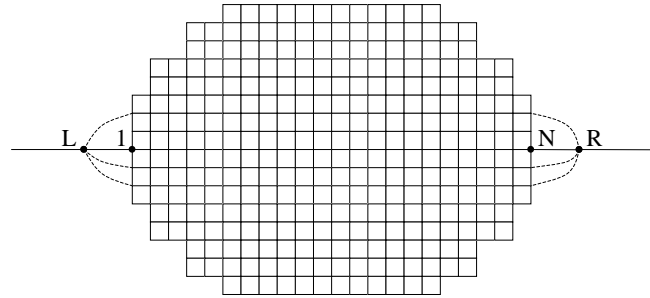


FIG. 1. Schematic representation of a lattice model for a quantum dot.

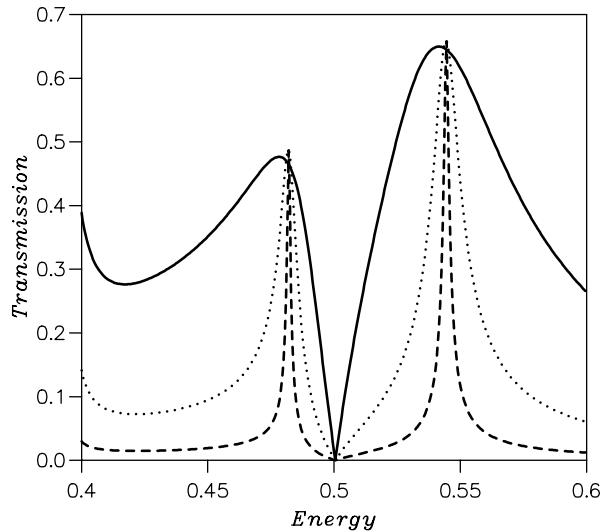


FIG. 2. Transmission probability versus energy for a 5x5 sites dot with  $\Gamma_L = \Gamma_R = 0.25$  (full line), 0.05 (dotted line) and 0.01 (broken line).

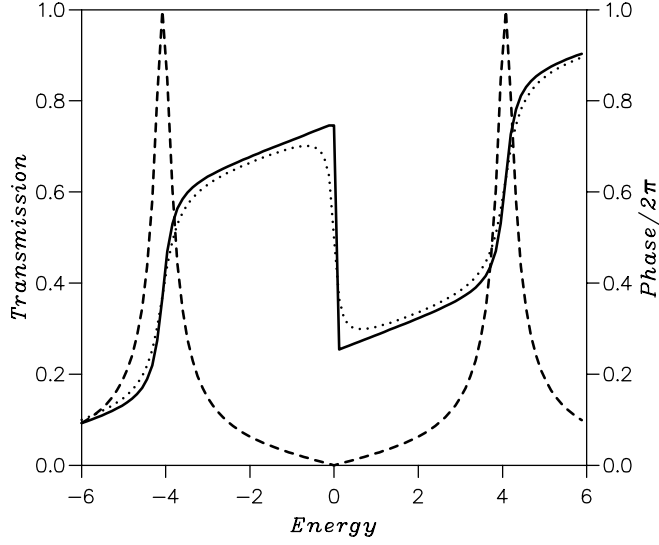


FIG. 3. Modulus (broken line) and phase (full line) of the transmission amplitude for a four sites dot given by Eq. (18) with  $\Gamma_L = \Gamma_R = 10$  and  $\epsilon_2 = -\epsilon_3 = 4$ . The dotted line shows corresponds to the phase when an inelastic tunneling rate  $\Gamma_{in} = 0.1$  is introduced.

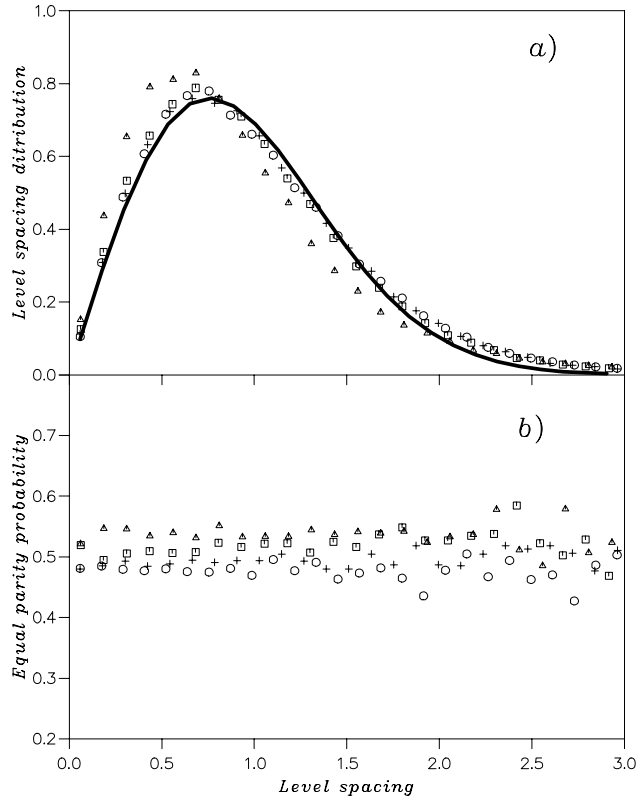


FIG. 4. Level spacing distribution and equal parity probability for a  $30 \times 30$  sites for different values of the disorder strength  $W$ : 0.5 (triangles), 1.0 (boxes), 2.0 (crosses) and 3.0 (circles). Full line corresponds to the Wigner distribution.

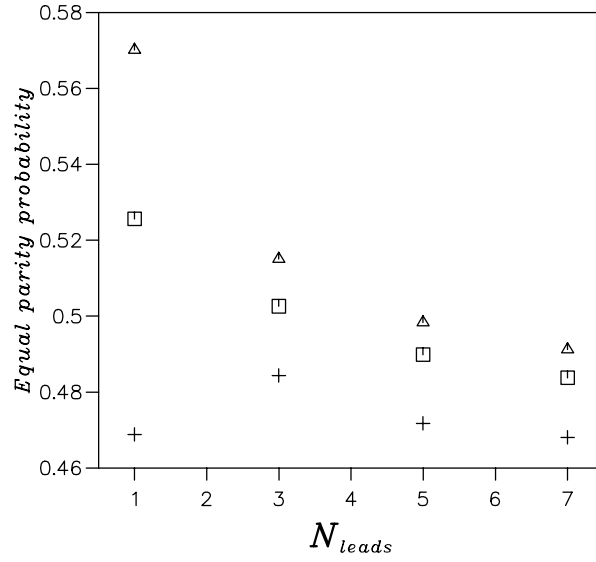


FIG. 5. Equal parity probability as a function of  $N_{leads}$  for  $W = 0.5$  (triangles),  $W = 1.0$  (boxes) and  $W = 2.0$  (crosses).

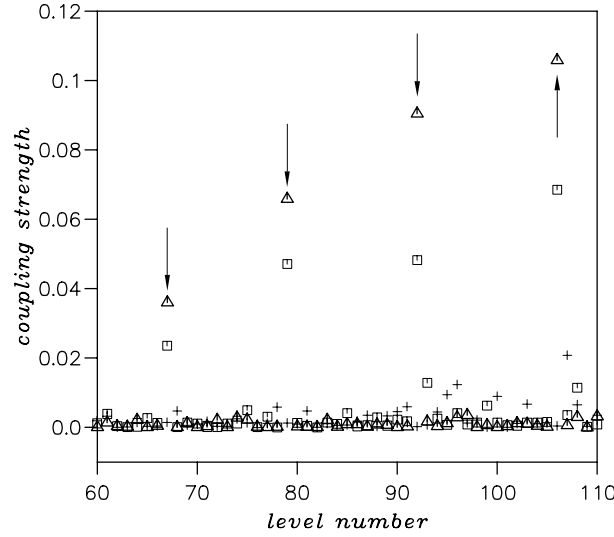


FIG. 6. Strength of the coupling to the leads  $\alpha_n$  as a function of level number for the case  $N_{leads} = 5$  and different values of  $W$ : 0.5 (triangles), 1.0 (boxes) and 2.0 (crosses). The arrows indicate states with the strongest coupling to the leads for the  $W = 0.5$  case.

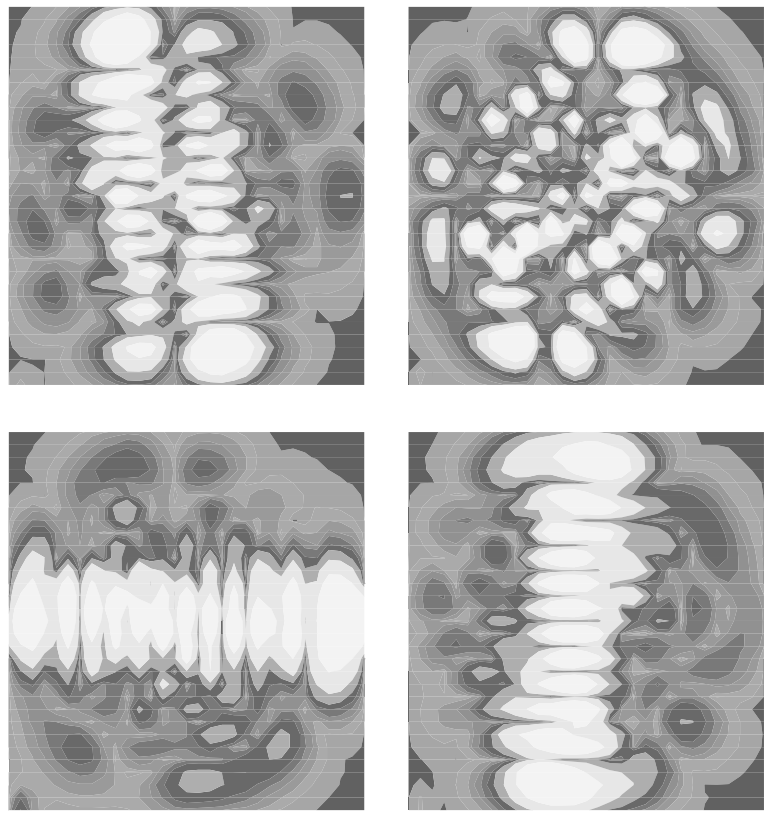


FIG. 7. Contour plots of the wavefunctions for the  $W = 0.5$  case corresponding (from bottom to top and from left to right) to level numbers 67, 68, 69 and 70.

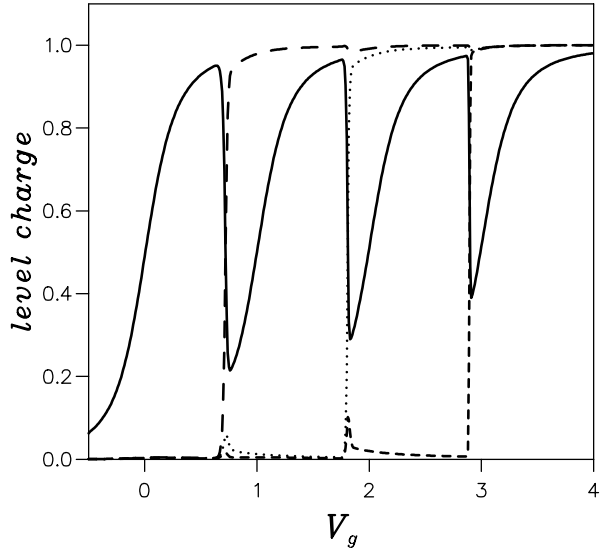


FIG. 8. Level charges as function of gate voltage for a 16 sites cluster (see parameters in text). The full line corresponds to the strongly coupled level and the dashed, dotted and small dashed lines correspond to the consecutive weakly coupled levels.

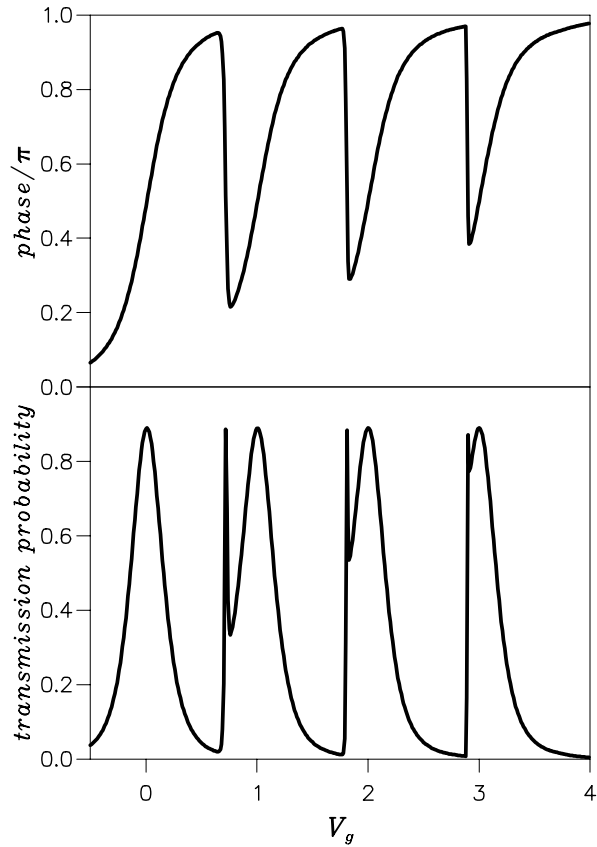


FIG. 9. Phase and modulus of the transmission amplitude for the model of Fig. 8 mapped into an effective one-electron problem.